



Contents lists available at ScienceDirect

Journal of Building Engineering

journal homepage: www.elsevier.com/locate/job

Influence of building thermal envelope modeling parameters on results of building energy simulation

Simon Muhič^{a, b, c, *}, Dimitrije Manić^d, Ante Čikić^e, Mirko Komatina^f

^a Institute for Renewable Energy and Efficient Exergy Use, INOVEKS, d.o.o., Cesta 2. Grupe odredov 17, 1295 Ivančna Gorica, Slovenia

^b Faculty of Industrial Engineering Novo mesto, Šegova ulica 112, 8000, Novo mesto, Slovenia

^c Rudolfovo - Science and Technology Centre Novo mesto, Podbreznik 15, 8000, Novo mesto, Slovenia

^d Innovation Center of Faculty of Mechanical Engineering, University of Belgrade, Kraljice Marije 16, 11120 Belgrade, Serbia

^e Department of Mechatronics, University North, 104. Brigade 3, 42000, Varaždin, Croatia

^f Faculty of Mechanical Engineering, University of Belgrade, Kraljice Marije 16, 11120 Belgrade, Serbia

ARTICLE INFO

Keywords:

Building energy modeling
Dynamic simulation
TRNSYS
Envelope modeling parameters
Building energy performance

ABSTRACT

The paper investigates the influence of input values for building energy model parameters on simulation results. The methodology is based on dynamic simulations in TRNSYS software, including models for three different buildings, with variations in different parameters such as referent dimensions, infiltration, envelope thermophysical properties, and thermal capacitance of interior space. The method is applied to a case study of theoretical buildings located in Slovenia. Obtained results suggest that the accuracy of model parameters' inputs related to thermal properties of glazing have the most significant impact on simulation results, where reduction in g-value from 0.62 to 0.22 reduces simulated $q_{H,nd}$ and $q_{C,nd}$ for 25% and 95% respectively. Referent dimensions for modeling floor area are the least influential parameter, where for Building III (BSF = 0.36) the change of referent dimensions results in variations of simulated $q_{H,nd}$ and $q_{C,nd}$ for less than $\pm 1\%$, while for Building I (BSF = 0.62) $q_{H,nd}$ and $q_{C,nd}$ variations are up to $\pm 20\%$. In general, for all model parameters, with a reduction of BSF, the influence of input variations is also reduced, meaning energy models for large buildings are more robust and less biased to deviation in simulation results from the inaccuracy of model inputs.

1. Introduction

The building sector is responsible for 40% of total final energy use and 36% of greenhouse gases (GHG) emissions in the European Union. About 60% of final energy use in the sector is estimated to be related to the operation of heating, cooling, and ventilation systems [1]. In households, the share of energy used for space conditioning and service water is even higher, with an estimated 70% of final energy used for heating, and 14% for preparing sanitary hot water [2]. In that context, European strategies and legislation set out a cross-sectional framework of targets for achieving high energy performance in buildings. The cornerstone of the regulatory framework was the first Energy Performance of Buildings Directive 2002/91/EC (EPBD), which set the commitment to reduce greenhouse gas emissions by 20% and increase the share of renewables in the energy mix to 20% by 2020. Subsequently, its recasts were provided in the form of European Directive 2010/31/EU and 2018/84/EU, aiming to further improve the energy efficiency of buildings across the European Union. The directives introduced various requirements including for new public buildings to be nearly Zero Energy Buildings (nZEBs) by 2018 and by 2020 for all new buildings. Overhaul, the European Union has set ambitious energy efficiency tar-

* Corresponding author. Institute for Renewable Energy and Efficient Exergy Use, INOVEKS, d.o.o., Cesta 2. Grupe odredov 17, 1295, Ivančna Gorica, Slovenia.
E-mail address: simon.muhic@inoveks.si (S. Muhič).

gets for 2030 as part of its broader climate and energy policy framework. These targets are outlined in the Clean Energy for All Europeans package, which includes several legislative initiatives aimed at advancing the EU's energy transition. This includes a target to achieve a 32.5% improvement in energy efficiency by 2030 compared to the 2007 baseline. This target was agreed upon as part of the EU's efforts to meet its commitments under the Paris Agreement and to contribute to the EU's overall climate goals. A 4.8% increase in energy use in buildings was estimated in 2021, surpassing the decline in 2020 (−2.5%), bringing final energy use in buildings back to 2017 levels [3]. Considering those recent energy use trends, it is going to be challenging for the EU to meet its energy efficiency target by 2030, i.e. 32.5% reduction in primary and final energy use compared to projections of expected energy use in 2030. Nevertheless, the European Commission has proposed amending the Energy Efficiency Directive with more ambitious targets for 2030, namely a 36% reduction in final energy use and a 39% reduction of primary energy to achieve carbon neutrality by 2050 [3].

The critical step in evaluating strategies and projects for increasing building energy efficiency is the assessment of building energy performance for existing buildings, as well as new construction and retrofit project. In this process, building energy simulation (BES) has an indispensable role. They complement the static calculations of buildings and are used to obtain data on energy use throughout the day, month, and year in buildings. Through simulations, we obtain information on the extent to which individual parameters affect the heating and cooling needs of the building. The obtained results enable us to build or rehabilitate existing buildings in an energy-optimal way.

BES can broadly be defined as a physics-based mathematical model that allows the detailed calculation of a building's energy performance and occupant thermal comfort under the influence of various inputs such as weather, building geometry, internal loads, HVAC systems, operational schedules, and simulation specific parameters. Originally intended for use during the design phase, BES is increasingly being used throughout a building's lifecycle [4]. However, there are increasing concerns about the credibility of building energy models within the building industry as significant discrepancies between simulated and measured energy use become apparent with the rapid deployment of smart energy meters and the Internet of things (IoT) [5]. Previous studies [6,7] observed that the main causes of discrepancies between predicted and actual energy performance stem from: (a) specification uncertainty arising from assumptions due to a lack of information; (b) model inadequacy arising from simplifications and abstractions of actual physical building systems; (c) operational uncertainty arising from a lack of feedback regarding actual use and operation of buildings; and (d) scenario uncertainty arising from specifying model conditions such as weather conditions and building occupancy.

EPBD primarily sets out requirements and objectives related to the energy performance of buildings, such as energy efficiency standards, renovation strategies, and the promotion of renewable energy use. While the directive does not specifically define building energy simulation procedures itself, it often encourages or mandates the use of building energy simulation tools to assess and improve the energy performance of buildings. EPBD doesn't directly define building energy simulation procedures, it provides a framework for promoting the use of such tools as part of efforts to improve the energy performance of buildings across the European Union.

In the last few years, the increased demand for energy simulations of buildings has led to the development of different computer programs for analyzing the dynamic response of buildings and the efficiency of systems. Building simulations are the first step towards high building energy efficiency. Today, software tools for energy modeling differ significantly from each other in the accuracy of model predictions and the level of complexity of preparing the analysis. That is why the European and international standards CEN and ISO are developed with the goal of international harmonization of the methodology for assessing the energy efficiency of buildings. In the field of energy efficiency, the ISO 50001 standard is important, which is based on continuous improvement, reducing energy costs, greenhouse gas emissions and reducing the negative impact on the environment. The ISO 50001 standard considers the PDCA approach (Plan-Do-Check-Act), which is used in the quality management system (ISO 9001) and environmental management (ISO 14001). Cholewa et al. confirmed the effectiveness of ISO 50001 as an organizational tool for energy management within a systematic approach [8].

In the past, the ISO 13790:2008 standard described calculation methods for assessing energy use in residential and non-residential buildings. In September 2017, ISO 52016-1:2017 replaced the ISO 13790:2008 standard. The new version also includes calculation methods for the assessment of energy required for space conditioning of residential or non-residential buildings. The ISO 52016-1:2017 standard was revised and approved in the summer of 2022, so it remains current.

A variety of BES software is currently available. In general, simulation tools can be divided into two main categories: tools based on dynamic simulation, and tools based on steady-state method. Wang et al. [9] provided a short description of dynamic simulation and steady-state methods and their applications. In the literature, we can also find a lot of mutual comparisons between them. Dermentzis et al. [10] compared the software PHPP (tool for energy assessment) and TRNSYS (tool for dynamic simulations) on 3 types of buildings (single-dwelling, multi-dwelling, non-dwelling), which were simulated before renovation and after renovation, based on weather data for 7 different European cities. To avoid mistakes, single-dwelling and multi-dwelling houses were defined as thermal zones in the TRNSYS software. Since PHPP uses two separate algorithms for calculating heating and cooling needs, two sets of simulations were also ordered in TRNSYS. The difference between both tools was a maximum of 3% for an existing residential building with a heating requirement of 25 kWh/m², and a maximum of 10% for a non-residential building. PHPP has proven to be a versatile tool that is a good alternative to more complex simulation tools that require more knowledge. In the TRNSYS software, the use of convective but operational temperature for monitoring heating and cooling had a negligible impact on the simulation of renovated buildings. However, in the case of existing buildings, the operating temperature caused significantly greater demands, especially for heating. PHPP does not differentiate between convective and operational temperature. For the calibration of PHPP, real data on the energy use of multi-residential buildings were obtained from the cost of fuel oil. Nageler et al. [11] performed a comparison of four simulation software tools: Dymola, EnergyPlus, IDA ICE and TRNSYS on a test model of a thermally active building system. The results were compared with the real results that were obtained with the test object and the results obtained in Ansys Fluent. TRNSYS and EnergyPlus had the lowest systematic and stochastic error. In general, they estimated the value deviation for all software tools Dymola

–0.92 K, EnergyPlus –2.18 K, IDA ICE –0.37 K and TRNSYS –1.13 K. Mangi et al. [12] performed a comparison of software tools: EnergyPlus, TRNSYS, IDA ICE, Modelica/Dymola, Matlab/Simulink, CarnotUIBK and ALMABuild, DALEC and PHPP on the example of a reference building (office) located in Rome, Stuttgart and Stockholm. They found that different tools require different levels of input details, which often do not match the available data, so the parameterization process strongly affects the quality of the simulation results. Other authors also compared different simulation tools [13–16].

BES software tools for dynamic simulation, developed in line with ISO standards and other relevant standards including CIBSE AM11 and ASHRAE 209–2018, are based on complex physical models that include a number of inputs related to geometry, architecture, thermophysical properties of the building envelope and interior spaces, and HVAC systems.

Building energy models are based on different assumptions related to building geometry, dimensions, or thermophysical properties. This is the case during early design stages for new construction or retrofit projects when energy modeling is an important part of the decision-making, yet the design details related to materials or geometry have not been finalized. This is also the case when modeling the energy performance of an existing building, since measuring and validating all thermophysical and geometry characteristics on site would be costly and time-consuming, therefore models are created based on educated assumptions or information from record drawings when available.

In practice, building energy simulation professionals are faced with various decisions related to the accuracy of the inputs. The higher the accuracy required for inputs, the more detailed design information is required from the engineers at various project stages, or more thorough field investigation for the existing buildings. This means that requirements for highly accurate inputs will significantly increase the resources required for BES process. Calleja et al. [17] proposed a methodology for sensitivity analysis (SA) related to the uncertainty of building energy model input parameters on a case study for a dwelling located in Spain and concluded only that weather and occupancy were the model parameters with the strongest influence of on simulated annual energy use.

Recently, Building Information Modelling based Building Energy Modelling (BIM-based BEM) is the approach gaining in popularity. This approach uses the pre-designed BIM model (including the information on architectural design and mechanical loads, materials' properties, and HVAC system) to create the input for BEM tools and provides an opportunity to make BEM a time-saving, low-cost, easy-to-use, more practical, consistent and accurate process. Designers can utilize the approach of BIM-based BEM to evaluate design options and make design decisions efficiently during the building design process, and the aim of building energy efficiency is easier to be achieved [18]. One of the questions related to the applicability of this approach at the pre-design stage is the relevance of simulation results, since building information and specifications, used to create an energy model during the pre-design, are usually re-defined at later stages of the design process.

Also, Adan et al. [19] showed that there is quite a challenging process to create a building energy simulation model from existing buildings or laser scanning to BES. Life Cycle Assessment of buildings is also based on BIM information [20,21].

The paper investigates the influence of inputs' variation for different building energy model parameters on simulation results, specifically the annual energy needed for heating and cooling. The methodology is based on building energy models and dynamic simulations in TRNSYS software, including models for three different buildings and 189 simulations in total. Model parameters for which input values have been varied through separate simulation sets include referent dimensions for modeled floor area, infiltration rate, windows area, frame factor (F_p), frame U-value, glazing U-value and g-value, external walls U-value and thermal bridging, and finally thermal capacity of interior spaces. The results and conclusions should help the building energy modeling professionals and researchers in making educated decisions when preparing building energy model input parameters, based on understanding the implications of their accuracy on simulation results.

2. Method

To conduct this study, baseline building models have been defined. The baseline building models are three buildings of different sizes, all located in Ljubljana, Slovenia. Building energy performance is simulated and quantified as the annual energy needed for heating ($q_{H,nd}$) and cooling ($q_{C,nd}$) per unit floor area of conditioned space. Simulation is performed using TRNSYS 18, which is based on the TFM (Transfer Function Method) dynamic simulation method, using weather data for a typical meteorological year for Ljubljana, obtained from the Slovenian meteorological agency. TRNSYS dynamic simulation uses weather and building data to solve a set of energy balance equations for every hour during the simulation period. The elements of the thermal envelope are modeled according to the transfer function relationships of Mitalas and Arseneault [22] defined from surface to surface, Fig. 2. For solar radiation Detailed Model - Gebhart Method is used.

2.1. Baseline building description

Three different buildings, in terms of size, are used for modeling and evaluation of the influence of all investigated modeling parameters. The difference between the three buildings is only the footprint dimensions, as presented in Table 1.

Table 1
Baseline building sizes.

Label	Footprint	Height	BSF
Building I	10 m × 10 m	9 m (three stories)	0.62
Building II	20 m × 20 m	9 m (three stories)	0.42
Building III	30 m × 30 m	9 m (three stories)	0.36

All baseline buildings have 20% window to floor ratio (Fig. 1). The baseline set of modeling parameters describing building thermophysical properties, including internal volume and thermal envelope has been defined to reflect a typical new construction building or energy retrofit projects in Slovenia. The same modeling parameters are used for Buildings I, II, and III. The baseline model external wall has U-value of $0.176 \text{ W/m}^2\text{K}$. Roof and slab floor on grade have U-values of $0.303 \text{ W/m}^2\text{K}$, and $0.145 \text{ W/m}^2\text{K}$ respectively. The baseline frame factor (F_F) for windows is 30%, with a frame U-value of $1.5 \text{ W/m}^2\text{K}$. The glazing is characterized by a U-value of $1.1 \text{ W/m}^2\text{K}$ and solar heat gain coefficient (g-value) of 0.62. The influence of thermal bridging and thermal capacitance of furniture are neglected for the baseline case, so only the thermal capacitance of air in thermal zone was modeled. Infiltration is modeled as a constant value of 0.5 ACH. The heating temperature setpoint is $20 \text{ }^\circ\text{C}$ and the cooling temperature setpoint is $26 \text{ }^\circ\text{C}$. Heating and cooling power were set as unlimited. On ground floor, identical boundary conditions were used.

Building floor area, and dimensions of the external walls are modeled per dimensions defining internal surfaces of exterior walls. Building envelope constructions are presented in Table 2, Table 3, and Table 4.

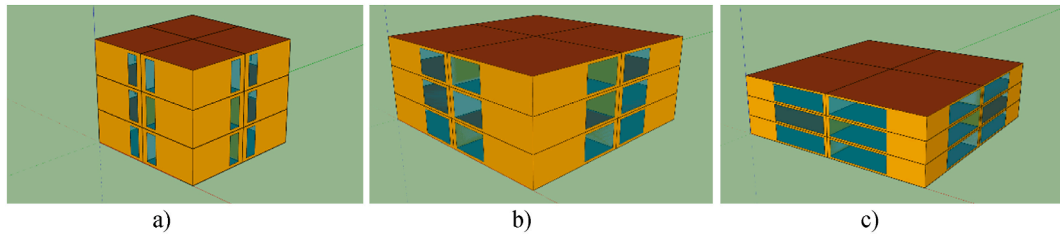


Fig. 1. Three baseline building sizes/geometries: a) $10 \times 10 \times 9 \text{ m}$; b) $20 \times 20 \times 9 \text{ m}$; c) $30 \times 30 \times 9 \text{ m}$.

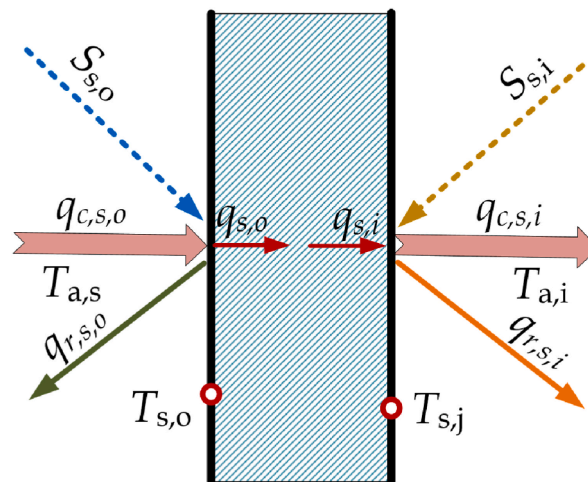


Fig. 2. Surface heat fluxes and temperatures [22].

Table 2

Thermophysical properties of exterior wall layers (total U-value = $0.176 \text{ W/m}^2\text{K}$; thickness 0.52 m).

	Thickness (m)	Density (kg/m^3)	Conductivity (W/mk)	Specific Heat (kJ/kgK)
Mortar1900	0.020	1900	3.564	1.05
Hollow Brick	0.290	1400	2.196	0.92
Mineral Wool	0.200	140	0.144	1.03
Mortar_ext	0.005	1550	2.520	1.05
Mortar Silikat	0.005	1550	2.520	1.05

Table 3

Slab floor on grade.

	Thickness (m)	Density (kg/m^3)	Conductivity (W/mk)	Specific Heat (kJ/kgK)
Parquet	0.020	700	0.756	1.67
Concrete2200	0.060	2200	5.436	0.96
XPS	0.100	35	0.137	1.50
Hydro insulation	0.010	1100	0.684	1.46

Table 4

Roof.	Thickness (m)	Density (kg/m ³)	Conductivity (W/mk)	Specific Heat (kJ/kgK)
Mortar1900	0.020	1900	3.564	1.05
Concrete2400	0.120	2200	5.436	0.96
Concrete2200	0.050	2200	7.344	0.96
Hydro insulation	0.010	1100	0.684	1.46
XPS	0.220	35	0.137	1.50
Gravel	0.080	1700	2.916	0.84

Energy balance equations in the simulation model include net radiative heat transfer $\dot{q}_{r,s,o}$ and $\dot{q}_{r,s,i}$ absorbed radiation heat fluxes $S_{s,o}$, $S_{s,i}$, conduction heat fluxes $\dot{q}_{s,o}$ and $\dot{q}_{s,i}$, and convection heat fluxes $\dot{q}_{c,s,o}$ and $\dot{q}_{c,s,i}$. The detailed description of the TRNSYS mathematical model is available at [22].

2.2. Variation of referent dimensions for modeled floor area

According to different industrial standards for building modeling (e.g. NECB 2017), the modeled floor area (MFA) must be within a specific percentage of gross floor area from the architectural drawings. Therefore, building model geometry is usually created based on dimensions between the outside of exterior walls. However, arguments can be made to account for internal dimensions, or the middle line (Fig. 3).

After the baseline buildings are created and their energy performance simulated, the first set of simulations with variation of input parameters is provided. It is provided for different referent dimensions defining building external walls and modeled floor area (MFA).

Furthermore, the modeling inputs defining infiltration rate are typically the number of air changes per hour (ACH), from which the infiltration airflow rate is calculated by simulation software, or an airflow rate (m³/h) calculated externally and provided as an input. So, when MFA is changed, this also changes the modeled volume of air inside the building, which affects the calculated infiltration airflow rate, if input is provided as the ACH value.

To illustrate the effect of inputs for model parameters defining MFA and infiltration on the simulated energy performance, simulations are provided for two typical approaches for modeling the infiltration. Namely, the approach where the input is the ACH (Table 5, Simulation ID x.1, x.2, x.4), and the approach where the infiltration volume flow rate is calculated and used as the input (Table 5, Simulation ID x.3, x.5) which is independent of MFA referent dimensions. Both approaches are tested on scenarios where referent MFA dimensions are internal, middle, and external lines of external walls.

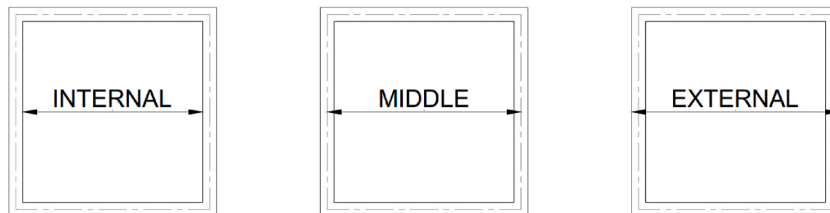


Fig. 3. Modeled floor area per internal, middle, or external dimensions.

Table 5

Building I, MFA dimensions and infiltration rates.

	Modeled dimensions	MFA [m ²]	Internal Volume [m ³]	ACH	Volume flow m ³ /h	Simulation ID
Building I	Internal	300.00	900.00	0.50	450	1.1
	Middle	332.01	996.03	0.50	498	1.2
				0.45	450	1.3
	External	365.65	1096.93	0.50	548	1.4
Building II				0.41	450	1.5
	Internal	1200	3600	0.50	1800	2.1
	Middle	1263	3790	0.50	1895	2.2
				0.47	1800	2.3
	External	1328	3984	0.50	1992	2.4
Building III				0.45	1800	2.5
	Internal	2700	8100	0.50	4050	3.1
	Middle	2794	8383	0.50	4192	3.2
				0.48	4050	3.3
	External	2890	8671	0.50	4336	3.4
			0.47	4050	3.5	

2.3. Variations of building envelope modeling parameters

Building envelope has a critical impact on building energy performance, which is recognized by all building energy standards and is the topic of numerous research efforts. Nevertheless, when creating a building simulation model exact specifications for building envelope elements, including external walls and windows, are usually not available. This refers to exact U-values for exterior walls, as well as windows' parameters including frame U-value, frame to window area, and glazing properties. Therefore, the model parameters for walls and windows are usually defined based on assumptions, using typical values for thermal transmittance (U-value) and solar heat gain coefficient (g-value). A set of simulations has been provided by varying parameters for external walls U-value, windows frame U-value, F_F , glazing U-value and g-value, and windows to floor ratio, as presented in Table 6. In each simulation, only one parameter is changed compared to the baseline.

2.4. Variation of thermal bridging

The effect of thermal bridges on building energy performance is significant, yet sometimes partially overlooked [23,24]. In TRN-SYS dynamic simulation, the impact of thermal bridges is considered by providing the value for linear or point thermal transmittances (ψ) of thermal bridges within the building envelope, which is in line with the methodology defining thermal bridging provided by the European Standard EN ISO 14683. Simulation set includes three variations with $\psi = 0$ W/mK (baseline), $\psi = 0,05$ W/mK, and $\psi = 0,10$ W/mK respectively (Table 7). The length of thermal bridges was 23 m (simulations 1.18 and 1.19), 43 m (simulations 2.18 and 2.19), and 63 m (simulations 3.18 and 3.19) per thermal zone.

2.5. Variation of interior space thermophysical properties

Furniture/indoor thermal mass has an impact on building energy flows and can affect energy efficiency [25]. The baseline energy models have been created with an interior space that contains only air, and no additional thermal mass. Additional simulations have been provided to assess how including the thermal capacity of furniture affects simulated building energy performance. In addition to the baseline condition, a simulation that includes wood furniture that occupies 1% and 2% of internal building volume respectively (Table 8). Wood density is 600 kg/m³ and the specific heat of wood 2.09 kJ/kgK.

3. Results and discussion

The presented simulation results focus on annual energy needs for heating and cooling per floor area and differences in results between the baseline building models and simulations with input parameter variations.

Table 6
Modeling parameters for external walls and windows.

Envelope Parameter	Value	Building I	Building II	Building III
		Simulation ID	Simulation ID	Simulation ID
Window to floor ratio	20%	1.1 (baseline)	2.1 (baseline)	2.1 (baseline)
	25%	1.6	2.6	2.6
	30%	1.7	2.7	2.7
Windows frame U-value	1.5 W/m ² K	1.1 (baseline)	2.1 (baseline)	2.1 (baseline)
	1.2 W/m ² K	1.8	2.8	2.8
	0.9 W/m ² K	1.9	2.9	2.9
Windows frame factor	30%	1.1	2.1	2.1
	25%	1.10	2.10	2.10
	20%	1.11	2.11	2.11
Glazing U-value (g=0.62)	1.10 W/m ² K	1.1 (baseline)	2.1 (baseline)	2.1 (baseline)
	0.88 W/m ² K	1.12	2.12	2.12
	0.62 W/m ² K	1.13	2.13	2.13
Glazing g-value (U=1.1 W/m²K)	0.62	1.1 (baseline)	2.1 (baseline)	2.1 (baseline)
	0.42	1.14	2.14	2.14
	0.22	1.15	2.15	2.15
External wall U-value	0.176 W/m ² K	1.1 (baseline)	2.1 (baseline)	2.1 (baseline)
	0.140 W/m ² K	1.16	2.16	2.16
	0.315 W/m ² K	1.17	2.17	2.17

Table 7
Modeling parameters for thermal bridges.

Envelope Parameter	Value	Building I	Building II	Building III
		Simulation ID	Simulation ID	Simulation ID
ψ	0 W/mK	1.1 (baseline)	2.1 (baseline)	3.1 (baseline)
	0,05 W/mK	1.18	2.18	3.18
	0,10 W/mK	1.19	2.19	3.19

Table 8
Modeling parameters for thermal capacitance.

Parameter	Value	Building I	Building II	Building III
		Simulation ID	Simulation ID	Simulation ID
Thermal capacitance	Air	1.1 (baseline)	2.1 (baseline)	3.1 (baseline)
	1% wood	1.20	2.20	3.20
	2% wood	1.21	2.21	3.21

The relative complexity of the model provides some counterintuitive results, such as an increase in annual energy needed for cooling when improving thermal insulation of building envelope elements. This is because most of the annual cooling loads are related to solar gains, not transmission gains. Often when the cooling loads occur based on solar gains, simultaneously outdoor air temperature is lower than the cooling setpoint (26 °C). Therefore, the heat flux through the wall is from the inside to the outside. So, increasing thermal insulation reduces the passive cooling effect and increases the energy needed for cooling.

3.1. Simulation results for variation of referent dimensions

In that context, the result presented in [Table 9](#), [Table 10](#), and [Table 11](#), show that the selection of referent dimensions for MFA (internal, middle, or external) can have a significant impact on energy performance assessment for buildings with smaller footprints and higher BSF. For Building I, which has a building shape factor of 0.62, the difference in simulated energy needed for heating and cooling is 19.61% and –19.28% respectively. As the building shape factor decreases, the influence of the choice of referent dimensions diminishes. Furthermore, if the modeling input for infiltration is the volume flow, which does not change with the selection of referent dimensions, then the difference of simulated energy performance is additionally reduced. Ultimately, for buildings with the largest footprint (Building III) and the smallest BSF, if infiltration input is the volume flow, even if the external dimensions are chosen as referent for MFA, the difference between simulated energy performance compared to the baseline is less than 1%.

Table 9
Building I simulation results for varying MFA and infiltration rate parameters.

Building I (10 × 10)					
Simulation ID	Description	$q_{H,nd}$ [kWh/m ²]	$\Delta q_{H,nd}$	$q_{C,nd}$ [kWh/m ²]	$\Delta q_{C,nd}$
1.1	internal; 0.5 ACH (450 m ³ /h)	52.49	Baseline	6.48	Baseline
1.2	middle; 0.5 ACH (498 m ³ /h)	57.51	9.57%	5.84	–9.92%
1.3	external; 0.5 ACH (548 m ³ /h)	62.78	19.61%	5.23	–19.28%
1.4	450 m ³ /h; middle	53.60	2.13%	6.31	–2.70%
1.5	450 m ³ /h; middle	54.75	4.31%	6.14	–5.37%

Table 10
Building II simulation results for varying MFA and infiltration rate parameters.

Building II (20 × 20)					
Simulation ID	Description	$q_{H,nd}$ [kWh/m ²]	$\Delta q_{H,nd}$	$q_{C,nd}$ [kWh/m ²]	$\Delta q_{C,nd}$
2.1	internal; 0.5 ACH (1800 m ³ /h)	45.51	Baseline	7.47	Baseline
2.2	middle; 0.5 ACH (1895 m ³ /h)	47.76	4.96%	7.12	–4.67%
2.3	external; 0.5 ACH (1992 m ³ /h)	50.08	10.05%	6.78	–9.18%
2.4	1800 m ³ /h; middle	45.86	0.77%	7.40	–0.91%
2.5	1800 m ³ /h; middle	46.21	1.56%	7.33	–1.81%

Table 11
Building III simulation results for varying MFA and infiltration rate parameters.

Building III (30 × 30)					
Simulation ID	Description	$q_{H,nd}$ [kWh/m ²]	$\Delta q_{H,nd}$	$q_{C,nd}$ [kWh/m ²]	$\Delta q_{C,nd}$
3.1	internal; 0.5 ACH (4050 m ³ /h)	43.28	Baseline	7.80	Baseline
3.2	middle; 0.5 ACH (4192 m ³ /h)	44.72	3.34%	7.57	–3.01%
3.3	external; 0.5 ACH (4336 m ³ /h)	46.19	6.74%	7.33	–5.98%
3.4	middle; 4050 m ³ /h; middle	43.46	0.43%	7.77	–0.46%
3.5	external; 4050 m ³ /h	43.65	0.87%	7.73	–0.92%

3.2. Simulation results for variations of windows parameters

The second set of simulations was related to variation of input parameters describing thermophysical properties and geometry of windows, as presented in Table 12, Table 13, and Table 14.

The results of simulations show that the strongest influential parameter is the SHGC (g-value), both for energy needed for heating and cooling. With g-value reduced from a baseline value of 0.62 to 0.22 the energy needed for heating is increased for 22% for Building I to 25% for Buildings II & III. The influence on simulated energy needed for cooling is even more significant, with a reduction of more than 90%.

Incremental changes of 5% for the window to floor ratio result in less than 1% incremental change of calculated annual energy for heating but have an extreme impact on calculated annual energy for cooling, which increases by about 50% for every 5% of a window to floor ratio increase.

Since the baseline windows frame factor is 30%, and window to floor ratio is 20%, this means that the windows frame accounts for only 3.21%, 4.47%, and 5.63% of the total envelope area for Buildings I, II, and III respectively. This illustrates why the frame U-value is the least influential factor, and an 18% improvement in frame U-value, results in only about 3% reduced energy needed for heating and about 5% change in calculated energy for cooling.

Table 12
Building I simulation results for varying parameters describing windows.

Building I (10 × 10)					
Simulation ID	Description	$q_{H,nd}$ [kWh/m ²]	$\Delta q_{H,nd}$	$q_{C,nd}$ [kWh/m ²]	$\Delta q_{C,nd}$
1.6	Window to floor 25%	52.20	-0.54%	10.19	57.20%
1.7	Window to floor 30%	52.18	-0.57%	14.30	120.51%
1.8	Frame U-value 1.2 W/m ² K	51.60	-1.69%	6.63	2.22%
1.9	Frame U-value 0.9 W/m ² K	50.69	-3.43%	6.78	4.55%
1.10	$F_F = 0.25$	51.33	-2.20%	7.60	17.22%
1.11	$F_F = 0.2$	50.21	-4.33%	8.79	35.57%
1.12	Glazing U-value 0.88 W/m ² K	47.91	-8.72%	6.90	6.44%
1.13	Glazing U-value 0.62 W/m ² K	45.86	-12.63%	7.22	11.30%
1.14	Glazing g-value 0.42	57.74	10.00%	2.04	-68.49%
1.15	Glazing g-value 0.22	64.51	22.91%	0.04	-99.37%

Table 13
Building II simulation results for varying parameters describing windows

Building II (20 × 20)					
Simulation ID	Description	$q_{H,nd}$ [kWh/m ²]	$\Delta q_{H,nd}$	$q_{C,nd}$ [kWh/m ²]	$\Delta q_{C,nd}$
2.6	Window to floor 25%	45.49	-0.04%	11.37	52.19%
2.7	Window to floor 30%	45.74	0.51%	15.53	107.96%
2.8	Frame U-value 1.2 W/m ² K	44.62	-1.94%	7.64	2.34%
2.9	Frame U-value 0.9 W/m ² K	43.72	-3.93%	7.83	4.80%
2.10	Frame ratio 25%	44.43	-2.37%	8.68	16.29%
2.11	Frame ratio 20%	43.39	-4.65%	9.96	33.42%
2.12	Glazing U-value 0.88 W/m ² K	40.93	-10.05%	7.98	6.81%
2.13	Glazing U-value 0.62 W/m ² K	38.89	-14.53%	8.38	12.17%
2.14	Glazing g-value 0.42	50.47	10.91%	2.64	-64.64%
2.15	Glazing g-value 0.22	56.94	25.13%	0.16	-97.84%

Table 14
Building III simulation results for varying parameters describing windows.

Building III (30 × 30)					
Simulation ID	Description	$q_{H,nd}$ [kWh/m ²]	$\Delta q_{H,nd}$	$q_{C,nd}$ [kWh/m ²]	$\Delta q_{C,nd}$
3.6	Window to floor 25%	43.37	0.23%	13.71	50.16%
3.7	Window to floor 30%	43.75	3.09%	15.85	103.18%
3.8	Frame U-value 1.2 W/m ² K	42.39	-2.05%	7.99	2.38%
3.9	Frame U-value 0.9 W/m ² K	43.48	-4.14%	8.18	4.88%
3.10	Frame ratio 25%	42.23	-2.42%	9.04	15.86%
3.11	Frame ratio 20%	43.22	-4.75%	10.34	32.50%
3.12	Glazing U-value 0.88 W/m ² K	38.69	-10.60%	8.34	6.92%
3.13	Glazing U-value 0.62 W/m ² K	36.64	-15.32%	8.78	12.50%
3.14	Glazing g-value 0.42	48.13	13.22%	2.83	-63.72%
3.15	Glazing g-value 0.22	54.47	25.88%	0.24	-96.98%

3.3. Simulation results for variations of external wall parameters

Results for the set of simulations related to variations of parameters defining external walls and thermal bridging are presented in Tables 15, 16 and 17. The results illustrate a significant and meaningful correlation between variation of those modeling inputs and variation of simulated building energy performance, especially for Building I with the highest BSF value. The reduced influence of envelope input parameters with a decrease of BSF is clearly illustrated at Fig. 6, where absolute values for $\Delta q_{H,nd}$ and $\Delta q_{C,nd}$ are 16%–18% for Building I with BSF of 0.62 and drop to below 5% for Building III with BSF of 0.36. This is due to the fact that with a reduction in BSF the total share of heat conduction and radiation through the envelope is reduced on account of the increased share of convective heat transfer (infiltration). The same would apply if other energy flows are considered, such as internal heat gains from lighting, people etc.

3.4. Simulation results for variation of internal volume thermal capacitance

Modeling the heat capacity of interior spaces is usually neglected in modeling practice, but the results presented in Table 18, Table 19, and Table 20 show that it should be considered especially when estimating the energy needed for cooling. This is also illustrated

Table 15
Building I simulation results for varying external wall parameters.

Building I (10 × 10)					
Simulation ID	Description	$q_{H,nd}$ [kWh/m ²]	$\Delta q_{H,nd}$	$q_{C,nd}$ [kWh/m ²]	$\Delta q_{C,nd}$
1.16	Ext. Wall U-value 0.140 W/m ² K	49.99	−4.75%	6.81	5.04%
1.17	Ext. Wall U-value 0.315 W/m ² K	62.27	18.64%	5.40	−16.72%
1.18	Thermal brid. $\psi = 0.05$ W/mK	55.79	6.31%	6.08	−6.25%
1.19	Thermal brid. $\psi = 0.10$ W/mK	59.11	12.63%	5.70	−12.03%

Table 16
Building III simulation results for varying external wall parameters.

Building II (20 × 20)					
Simulation ID	Description	$q_{H,nd}$ [kWh/m ²]	$\Delta q_{H,nd}$	$q_{C,nd}$ [kWh/m ²]	$\Delta q_{C,nd}$
2.16	Ext. Wall U-value 0.140 W/m ² K	44.52	−2.17%	7.63	2.16%
2.17	Ext. Wall U-value 0.315 W/m ² K	49.38	8.52%	6.90	−7.65%
2.18	Thermal brid. $\psi = 0.05$ W/mK	47.04	3.36%	7.24	−3.06%
2.19	Thermal brid. $\psi = 0.10$ W/mK	48.57	6.73%	7.02	−5.98%

Table 17
Building III simulation results for varying external wall parameters.

Building III (30 × 30)					
Simulation ID	Description	$q_{H,nd}$ [kWh/m ²]	$\Delta q_{H,nd}$	$q_{C,nd}$ [kWh/m ²]	$\Delta q_{C,nd}$
3.16	Ext. Wall U-value 0.140 W/m ² K	42.78	−3.14%	7.89	3.10%
3.17	Ext. Wall U-value 0.315 W/m ² K	45.21	4.46%	7.48	−4.05%
3.18	Thermal brid. $\psi = 0.05$ W/mK	44.27	2.29%	7.64	−2.02%
3.19	Thermal brid. $\psi = 0.10$ W/mK	45.26	4.59%	7.49	−3.98%

Table 18
Building I simulation results for varying thermal capacitance of thermal zones.

Building I (10 × 10)					
Simulation ID	Description	$q_{H,nd}$ [kWh/m ²]	$\Delta q_{H,nd}$	$q_{C,nd}$ [kWh/m ²]	$\Delta q_{C,nd}$
1.20	Heat capacity, 1% vol. Furniture	52.44	−0.09%	6.41	−1.11%
1.21	Heat capacity, 2% vol. Furniture	52.39	−0.17%	6.34	−2.24%

Table 19
Building II simulation results for varying thermal capacitance of thermal zones.

Building II (20 × 20)					
Simulation ID	Description	$q_{H,nd}$ [kWh/m ²]	$\Delta q_{H,nd}$	$q_{C,nd}$ [kWh/m ²]	$\Delta q_{C,nd}$
3.16	Heat capacity, 1% vol. Furniture	45.45	−0.12%	7.37	−1.35%
3.17	Heat capacity, 2% vol. Furniture	45.39	−0.24%	7.27	−2.70%

Table 20

Building III simulation results for varying thermal capacitance of thermal zones.

Building III (30 × 30)					
Simulation ID	Description	$q_{H,nd}$ [kWh/m ²]	$\Delta q_{H,nd}$	$q_{C,nd}$ [kWh/m ²]	$\Delta q_{C,nd}$
3.16	Heat capacity, 1% vol. Furniture	43.22	-0.14%	7.69	-1.43%
3.17	Heat capacity, 2% vol. Furniture	43.16	-0.28%	7.58	-2.84%

in Fig. 7 which shows that for 1% incremental increase of increase in furniture volume to total internal volume ratio, the energy need for cooling also decreases by about 1%. This is basically because part of solar gains, which are related to short periods of the day, are stored in the furniture thermal mass, and then gradually removed through passive cooling by convection and radiation in periods when cooling peak demand has passed and indoor air temperature is already below the cooling setpoint.

4. Conclusions

This paper presents a study investigating the influence of building energy model parameters' input value variations on the results of dynamic simulation, specifically the annual energy needed for heating and annual energy needed for cooling. The study is conducted on examples of buildings located in Ljubljana, Slovenia. The results indicate that the influence of input variations could be significant and in general, it is reduced with an increase in building size (reduction of building shape factor).

Perhaps somewhat counterintuitively, the most influential building envelope parameter for both heating and cooling energy simulation is the glazing solar heat gain coefficient (g-value). Reducing the g-value from a baseline value of 0.62 to 0.22 leads to a relative increase in energy needed for heating of about 25% and a reduction in energy needed for cooling of more than 95%.

The simulated energy performance is less affected by parameters defining conduction through the envelope, compared to parameters defining convective heat transfer by infiltration, or radiative heat transfer through windows. Changing windows frame U-value from 1.1 W/m²K to 0.9 W/m²K and 1.2 W/m²K respectively results in changes of $q_{H,nd}$ and $q_{C,nd}$ for only up to $\pm 5\%$. Related to convective heat transfer, depending on which combination of parameters are selected for modeling infiltration (ACH vs air volume flow) and floor area of the conditioned space, $q_{H,nd}$ and $q_{C,nd}$ can be $\pm 20\%$ different compared to the baseline (Table 9, Table 10, Table 11 and Fig. 4) for the building with higher BSF. The deviation from the baseline is reduced to only about $\pm 6\%$ for larger buildings with lower BSF.

When modeling windows, the most influential parameters for both heating and cooling energy simulation are glazing U-value and g-value. Variation of input values for those parameters leads to significant deviations in $q_{H,nd}$ and $q_{C,nd}$ as presented in Table 12, Table 13, and Table 14, and illustrated on Fig. 5.

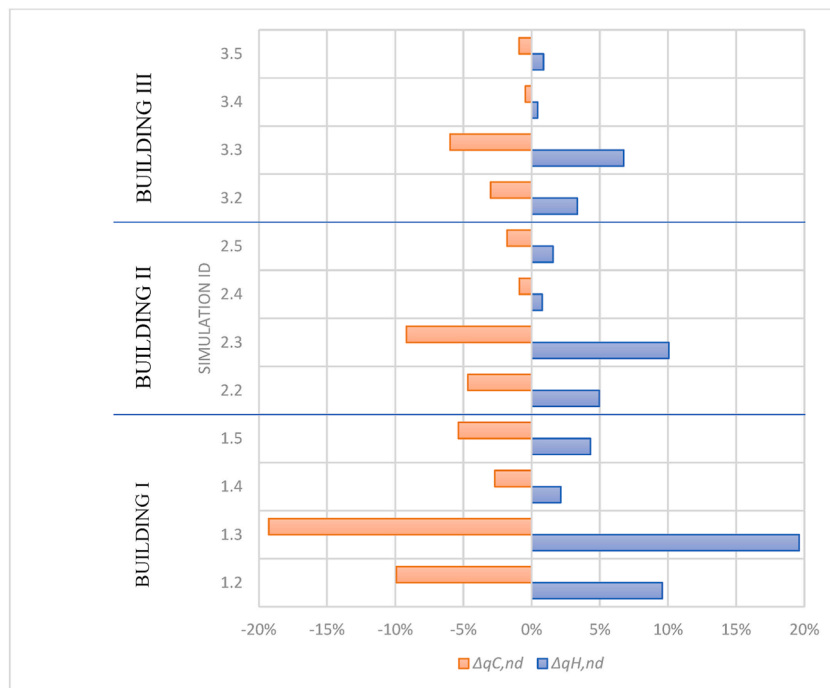


Fig. 4. Correlation between referent MFA dimensions and relative change in simulated energy performance.

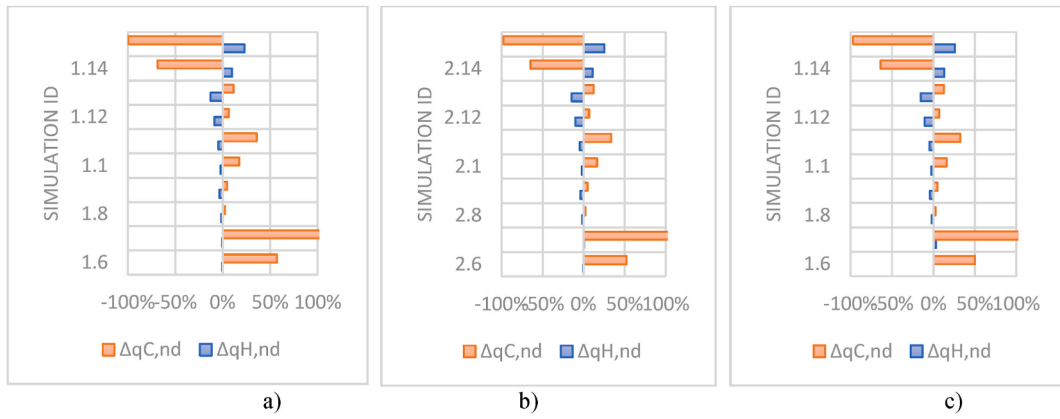


Fig. 5. Correlation between model windows parameters and relative change in simulated energy performance.

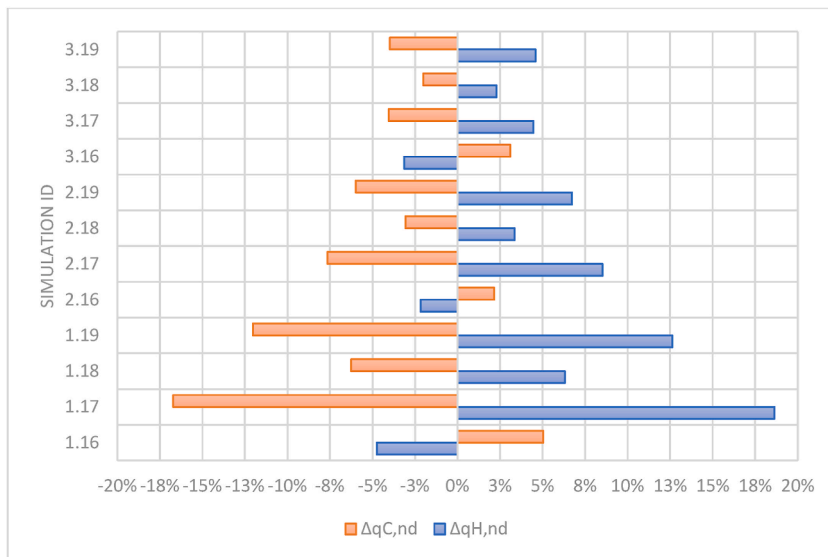


Fig. 6. Correlation between model external wall parameters and relative change in simulated energy performance.

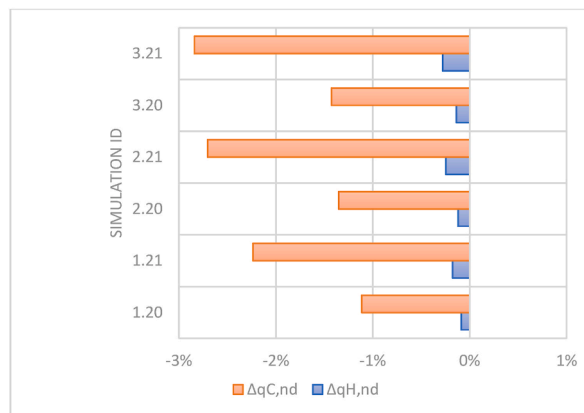


Fig. 7. Correlation between model thermal capacitance of thermal zones and relative change in simulated energy performance.

In general, all variations in inputs for building envelope model parameters have a more significant influence for buildings with higher BSF (Building I), and a lower impact for buildings with lower BSF (Building III).

Furthermore, results also show that interior space thermophysical properties should be taken into consideration when creating building energy models, especially in relation to energy flows for cooling. The values presented in Table 18, Table 19, Table 20, and Fig. 7 indicate that unlike for the building envelope parameters, the correlation between the thermal capacity of interior spaces and simulated energy performance, is even more significant for buildings with lower BSF (larger volume), especially for the annual energy needed for cooling.

It is important to point out that the modeled building energy flows include conductive and radiative heat transfer through the building envelope, convective heat transfer through infiltration, as well as heating and cooling equipment. Other energy flows, including mechanical and natural ventilation and internal heat gains are not part of the analysis.

Having that in mind, the findings from this paper need to be interpreted and implemented contextually, when phenomena like ventilation or internal gains are included in the model. However, the implication of including additional energy flows in the model can be only the reduction of the quantitative influence of variation of modeling parameters on simulation results, but the nature of correlation will be similar to what is presented in this paper.

CRedit authorship contribution statement

Simon Muhić: Conceptualization, Formal analysis, Methodology, Supervision, Writing – original draft, Writing – review & editing, Validation. **Dimitrije Manić:** Conceptualization, Formal analysis, Investigation, Methodology, Visualization, Writing – original draft, Writing – review & editing. **Ante Čikić:** Conceptualization, Methodology, Supervision, Writing – review & editing. **Mirko Komatina:** Conceptualization, Methodology, Supervision, Writing – review & editing.

Declaration of competing interest

The authors declare that they have no known competing financial interests or personal relationships that could have appeared to influence the work reported in this paper

Data availability

No data was used for the research described in the article.

Acknowledgements

This research was supported by the Science Fund of the Republic of Serbia, Project No. 4344, Grant No. TF C1389YF, “Forward Looking Framework for Accelerating Households” Green Energy Transition – FF GreEN.

Nomenclature

ACH	Number of air changes per hour
BSF	Building shape factor
F_F	Frame factor
g	Total solar energy transmittance of the transparent part of the element
I_{sol}	Annual solar irradiance, per unit area of collecting area of surface ($W\cdot m^{-2}$)
U	Thermal transmittance ($W\cdot m^{-2}K^{-1}$)
$Q_{H,nd}$	Annual energy need for heating per unit floor area of conditioned space ($kWh\cdot m^{-2}$)
$Q_{C,nd}$	Annual energy need for cooling per unit floor area of conditioned space ($kWh\cdot m^{-2}$)
$\dot{q}_{c,s,i}$	Convection heat flux from the inside surface to the air
$\dot{q}_{c,s,o}$	Convection heat flux to the outside surface from the boundary/ambient
$\dot{q}_{r,s,i}$	Net radiative heat transfer with all other surfaces within the zone
$\dot{q}_{r,s,o}$	Net radiative heat transfer with all surfaces in view of the outside surface
$\dot{q}_{s,i}$	Conduction heat flux from the wall at the inside surface
$\dot{q}_{s,o}$	Into the wall at the outside surface
$S_{s,i}$	Radiation heat flux absorbed at the inside surface (solar gains and radiative gains)
$S_{s,o}$	Radiation heat flux absorbed at the outside surface (solar gains)

References

- [1] M. Bošnjaković, M. Katinić, A. Čikić, S. Muhić, Building integrated photovoltaics. Overview of barriers and opportunities, *Therm. Sci.* 27 (2023) 1433–1451, <https://doi.org/10.2298/TSCI221107030B>.
- [2] S. Muhić, M. Šturm, M. Mazej, Numerical and experimental validation of low exergy system for heating and cooling of residential buildings, *Int. J. Eng. Adv. Technol.* 2 (2013) 345–352. <https://www.ijeat.org/portfolio-item/E1869062513/>.
- [3] Primary and Final Energy Consumption in Europe (8th EAP), Eur. Environment Agency, 2022.
- [4] J.L.M. Hensen, R. Lamberts, *Building Performance Simulation for Design and Operation*, second ed., Routledge, 2019.
- [5] P. De Wilde, The gap between predicted and measured energy performance of buildings: a framework for investigation, *Autom. ConStruct.* 41 (2014) 40–49, <https://doi.org/10.1016/J.AUTCON.2014.02.009>.
- [6] S. De Wit, G. Augenbroe, Analysis of uncertainty in building design evaluations and its implications, *Energy Build.* 34 (2002) 951–958, <https://doi.org/10.1016/>

- S0378-7788(02)00070-1.
- [7] A.C. Menezes, A. Cripps, D. Bouchlaghem, R. Buswell, Predicted vs. actual energy performance of non-domestic buildings: using post-occupancy evaluation data to reduce the performance gap, *Appl. Energy* 97 (2012) 355–364, <https://doi.org/10.1016/J.APENERGY.2011.11.075>.
 - [8] T. Cholewa, C.A. Balaras, S. Nižetić, A. Siuta-Olcha, On calculated and actual energy savings from thermal building renovations – long term field evaluation of multifamily buildings, *Energy Build.* 223 (2020) 110145, <https://doi.org/10.1016/j.enbuild.2020.110145>.
 - [9] S. Wang, C. Yan, F. Xiao, Quantitative energy performance assessment methods for existing buildings, *Energy Build.* 55 (2012) 873–888, <https://doi.org/10.1016/J.ENBUILD.2012.08.037>.
 - [10] G. Dermentzis, F. Ochs, M. Gustafsson, T. Calabrese, D. Siegele, W. Feist, C. Dipasquale, R. Fedrizzi, C. Bales, A comprehensive evaluation of a monthly-based energy auditing tool through dynamic simulations, and monitoring in a renovation case study, *Energy Build.* 183 (2019) 713–726, <https://doi.org/10.1016/j.enbuild.2018.11.046>.
 - [11] P. Nageler, G. Schweiger, M. Pichler, D. Brandl, T. Mach, R. Heimrath, H. Schranzhofer, C. Hochenauer, Validation of dynamic building energy simulation tools based on a real test-box with thermally activated building systems (TABS), *Energy Build.* 168 (2018) 42–55, <https://doi.org/10.1016/j.enbuild.2018.03.025>.
 - [12] M. Mangi, F. Ochs, S. de Vries, A. Maccarini, F. Sigg, Detailed cross comparison of building energy simulation tools results using a reference office building as a case study, *Energy Build.* 250 (2021), <https://doi.org/10.1016/j.enbuild.2021.111260>.
 - [13] D.B. Crawley, J.W. Hand, M. Kummert, B.T. Griffith, Contrasting the capabilities of building energy performance simulation programs, *Build. Environ.* 43 (2008) 661–673, <https://doi.org/10.1016/j.buildenv.2006.10.027>.
 - [14] D. Connolly, H. Lund, B.V. Mathiesen, M. Leahy, A review of computer tools for analysing the integration of renewable energy into various energy systems, *Appl. Energy* 87 (2010) 1059–1082, <https://doi.org/10.1016/j.apenergy.2009.09.026>.
 - [15] A. Gelesz, E. Catto Lucchino, F. Goia, V. Serra, A. Reith, Characteristics that matter in a climate façade: a sensitivity analysis with building energy simulation tools, *Energy Build.* 229 (2020) 110467, <https://doi.org/10.1016/j.enbuild.2020.110467>.
 - [16] D. Mazzeo, N. Matera, C. Cornaro, G. Olivetti, P. Romagnoni, L. De Santoli, EnergyPlus, IDA ICE and TRNSYS predictive simulation accuracy for building thermal behaviour evaluation by using an experimental campaign in solar test boxes with and without a PCM module, *Energy Build.* 212 (2020) 109812, <https://doi.org/10.1016/j.enbuild.2020.109812>.
 - [17] G. Calleja Rodríguez, A. Carrillo Andrés, F. Domínguez Muñoz, J.M. Cejudo López, Y. Zhang, Uncertainties and sensitivity analysis in building energy simulation using macroparameters, *Energy Build.* 67 (2013) 79–87, <https://doi.org/10.1016/J.ENBUILD.2013.08.009>.
 - [18] H. Gao, C. Koch, Y. Wu, Building information modelling based building energy modelling: a review, *Appl. Energy* 238 (2019) 320–343, <https://doi.org/10.1016/J.APENERGY.2019.01.032>.
 - [19] A. Adán, A. Ramón, J.L. Vivancos, A. Vilar, C. Aparicio-Fernández, Automatic generation of as-is BEM models of buildings, *J. Build. Eng.* 73 (2023) 106865, <https://doi.org/10.1016/J.JOBE.2023.106865>.
 - [20] M. Motalebi, A. Rashidi, M.M. Nasiri, Optimization and BIM-based lifecycle assessment integration for energy efficiency retrofit of buildings, *J. Build. Eng.* 49 (2022) 104022, <https://doi.org/10.1016/J.JOBE.2022.104022>.
 - [21] B. Soust-Verdaguer, I. Bernardino Galeana, C. Llatas, M.V. Montes, E. Hoxha, A. Passer, How to conduct consistent environmental, economic, and social assessment during the building design process. A BIM-based Life Cycle Sustainability Assessment method, *J. Build. Eng.* 45 (2022) 103516, <https://doi.org/10.1016/J.JOBE.2021.103516>.
 - [22] S.A. Klein, W.A. Beckman, J.W. Mitchell, J.A. Duffie, N.A. Duffie, T.L. Freeman, J.C. Mitchell, J.E. Braun, B.L. Evans, J.P. Kummer, R.E. Urban, A. Fiksel, J.W. Thornton, N.J. Blair, P.M. Williams, D.E. Bradley, T.P. McDowell, M. Kummert, D.A. Arias, M.J. Duffy, TRNSYS 18: a Transient System Simulation Program, Solar Energy Laboratory, University of Wisconsin, Madison, USA, 2017.
 - [23] H. Ge, F. Baba, Dynamic effect of thermal bridges on the energy performance of a low-rise residential building, *Energy Build.* 105 (2015) 106–118, <https://doi.org/10.1016/J.ENBUILD.2015.07.023>.
 - [24] S.A. Al-Sanea, M.F. Zedan, Effect of thermal bridges on transmission loads and thermal resistance of building walls under dynamic conditions, *Appl. Energy* 98 (2012) 584–593, <https://doi.org/10.1016/J.APENERGY.2012.04.038>.
 - [25] H. Johra, P. Heiselberg, Influence of internal thermal mass on the indoor thermal dynamics and integration of phase change materials in furniture for building energy storage: a review, *Renew. Sustain. Energy Rev.* 69 (2017) 19–32, <https://doi.org/10.1016/J.RSER.2016.11.145>.